Biochemical and Biophysical Research Communications 514 (2019) 1108–1114

Contents lists available at ScienceDirect

Biochemical and Biophysical Research Communications

journal homepage: www.elsevier.com/locate/ybbrc

# Structural insights into the catalysis and substrate specificity of cyanobacterial aspartate racemase McyF

Dong-Dong Cao [1], Chun-Peng Zhang [1], Kang Zhou, Yong-Liang Jiang, Xiao-Feng Tan, Jin Xie, Yan-Min Ren, Yuxing Chen, Cong-Zhao Zhou, Wen-Tao Hou*

*Hefei National Laboratory for Physical Sciences at the Microscale and School of Life Sciences, University of Science and Technology of China, Hefei Anhui 230027, China*

ARTICLE INFO

*Article history:*
Received 30 April 2019
Accepted 7 May 2019
Available online 14 May 2019

*Keywords:*
Amino acids enantiomers
Racemase
Crystal structure
Racemization activity
Substrate specificity

ABSTRACT

L-amino acids represent the most common amino acid form, most notably as protein residues, whereas D-amino acids, despite their rare occurrence, play significant roles in many biological processes. Amino acid racemases are enzymes that catalyze the interconversion of L- and/or D-amino acids. McyF is a pyridoxal 5′-phosphate (PLP) independent amino acid racemase that produces the substrate D-aspartate for the biosynthesis of microcystin in the cyanobacterium *Microcystis aeruginosa* PCC7806. Here we report the crystal structures of McyF in complex with citrate, L-Asp and D-Asp at 2.35, 2.63 and 2.80 Å, respectively. Structural analyses indicate that McyF and homologs possess highly conserved residues involved in substrate binding and catalysis. In addition, residues Cys87 and Cys195 were clearly assigned to the key catalytic residues of "two bases" that deprotonate D-Asp and L-Asp in a reaction independent of PLP. Further site-directed mutagenesis combined with enzymatic assays revealed that Glu197 also participates in the catalytic reaction. In addition, activity assays proved that McyF could also catalyze the interconversion of L-MeAsp between D-MeAsp, the precursor of another microcystin isoform. These findings provide structural insights into the catalytic mechanism of aspartate racemase and microcystin biosynthesis.



## 1. Introduction

All α-amino acids but glycine exist in either of the two enantiomers, termed D- and L-enantiomers. L-amino acids represent the most common form of protein residues, whereas D-amino acids play significant roles in many biological processes despite their rare occurrence. For instance, the bacterial D-glutamic acid and D-alanine are essential components of cell-wall peptidoglycan [1,2]. The mammalian D-serine is a neuromodulator and D-aspartate is indispensable for fetal brain development [3,4]. Amino acid racemases catalyze the production of D-amino acid from its L-form, either dependent on or independent of the cofactor pyridoxal 5′-phosphate (PLP). For PLP-independent amino acid racemases, such as glutamate, proline, and aspartate racemases [5], it was proposed that two conserved cysteines work as the catalytic acids/bases [6]. Notably, recent reports of *Escherichia coli* aspartate/glutamate racemase crystal structures suggested that Thr83/Cys197, instead of two cysteines, function as the catalytic residues [7,8]. However, the fine catalytic mechanism and substrate specificity of amino acid racemases remain unclear.

The biosynthesis of microcystin in *Microcystis aeruginosa* PCC7806 is catalyzed by a series of proteins encoded by the *mcy* gene cluster [9,10]. McyF, which is encoded by *mcyF* gene, was reported to be an aspartate racemase [11]. In fact, *M. aeruginosa* PCC7806 produces two isoforms of microcystin, which employ either D-Asp or D-β-methyl-aspartate (D-MeAsp) as the precursor [12]. D-Asp has been proved to be the product of McyF from L-Asp [11]; however, whether McyF contributes to the generation of another precursor D-MeAsp remains unclear. Moreover, there is no direct evidence for the substrate specificity and catalytic mechanism of McyF.

Here we determined the crystal structures of McyF in complex with citrate, L-Asp and D-Asp, respectively. These structures enabled us to assign Cys87 and Cys195 to function as the previously proposed "two bases" [6]. In addition, the highly conserved residue Glu197 was identified to assist Cys195 in the racemase reaction of

* Corresponding author.
*E-mail address:* todvince@mail.ustc.edu.cn (W.-T. Hou).
[1] These authors contribute equally to this work.

https://doi.org/10.1016/j.bbrc.2019.05.063
0006-291X/

the interconversion of L-Asp and D-Asp. Furthermore, with biochemical assays we proved that McyF is capable of catalyzing the interconversion of L-MeAsp and D-MeAsp.

## 2. Materials and methods

### 2.1. Cloning, expression and purification

The coding sequence of McyF was amplified from the genomic DNA of *M. aeruginosa* PCC 7806, cloned into a pET-28a-derived expression vector (Novagen) with an N-terminal 6 × His tag and overexpressed in *E. coli* strain BL21 (DE3) (Novagen) using 2 × YT culture medium with 30 μg/mL kanamycin. Bacteria were grown at 37 °C to an absorbance of 0.8 at 600 nm and then induced with 0.2 mM isopropyl-β-D-1-thiogalactopyranoside for an additional 4 h. The bacteria were harvested and resuspended with lysis buffer (20 mM Tris-HCl pH 7.5, 200 mM NaCl). After sonication for 20 min followed by centrifugation, the supernatant containing the soluble protein was loaded onto a Ni-NTA column (GE healthcare) equilibrated with the binding buffer (20 mM Tris-HCl pH 7.5, 200 mM NaCl). The target protein was eluted with 400 mM imidazole, and further loaded onto a Superdex 75 column (GE Healthcare) pre-equilibrated with 20 mM Tris-HCl pH 7.5, 200 mM NaCl, 14 mM β-mercaptoethanol. Fractions containing the target protein were pooled and concentrated to 10 mg $mL^{-1}$ for crystallization.

Site-directed mutagenesis was performed using the PCR-based site-directed mutagenesis with the plasmid encoding the wild-type McyF as the template.

Seleno-methionine (SeMet) substituted McyF was expressed in *E. coli* strain B834 (DE3) (Novagen). The cells were harvested when the $A_{600nm}$ reached 0.2 and were then washed twice with M9 medium [13]. The cells were then cultured in SeMet medium (M9 medium with 25 μg $mL^{-1}$ L-SeMet and 50 μg $mL^{-1}$ other essential amino acids) containing 30 μg $mL^{-1}$ kanamycin to the absorbance of 0.8 at 600 nm. The remaining steps were the same as those for native McyF.

The coding sequence of human D-aspartate oxidase (hDDO) was synthetized by Sangon Biotech (Shanghai). Recombinant hDDO containing N-terminally His-tagged was cloned into the pET28a expression vector (Novagen) and expressed in *E. coli* strain BL21 (DE3) (Novagen) using 2 × YT culture medium with 30 μg/mL kanamycin. The remaining steps of protein expression, purification, storage of hDDO were the same as those for native McyF.

### 2.2. Crystallization, data collection and processing

Screening for the crystallization conditions of McyF and mutants was performed using screening kits of Crystal Screen I and II, Index, Grid screens and SaltRx (Hampton Research) with the hanging drop vapor-diffusion method at 16 °C. Crystals of SeMet-substituted McyF were grown with the initial condition of mixing 1 μL protein sample with an equal volume of reservoir solution (25% (w/v) polyethylene glycol 3350, 0.1 M sodium citrate, pH 6.5, 0.2 M $MgCl_2$) against 0.5 mL reservoir solution. Crystals of McyF-C87S/C195S in complex with L-Asp or D-Asp (20 mM, Sigma-Aldrich) were obtained by the same technique within a reservoir solution (25% (w/v) polyethylene glycol 3350, 0.2 M $MgCl_2$). The X-ray diffraction data were collected at 100 K using beamline BL17U with an ADSC Q315r CCD detector and beamline BL18U with a DECTRIS PILATUS 6 M PIXEL detector at Shanghai Synchrotron Radiation Facility (SSRF). All diffraction data were indexed, integrated, and scaled with the program HKL2000 [14].

### 2.3. Structure determination and refinement

The crystal structure of SeMet-substituted McyF was determined by the single-wavelength anomalous dispersion (SAD) phasing method. The AutoSol program from PHENIX [15] was used to locate the selenium atoms and to calculate the initial phases. Automatic model building was carried out using AutoBuild in PHENIX. Afterwards, the initial model was used for the molecular replacement process against the other three data sets with MOLREP. Refinement was carried out using CCP4i program suite [16] and the model was rebuilt using the program COOT [17]. The final model was evaluated with MOLPROBITY [18] and PROCHEK [19]. Crystallographic parameters, data collection statistics, and refinement statistics are listed in Table 1. All figures showing structures were prepared with PyMOL (http://www.pymol.org).

### 2.4. Enzymatic assays

The specific relative activities of McyF and mutants toward L-Asp (D-Asp) were determined as previously described [20] with minor modifications. Specifically, for L-Asp, the standard assay mixture contained McyF or mutants (600 nM), sodium pyrophosphate buffer (pH 8.0; 40 mM), catalase (5 μg), hDDO (1500 nM) and L-Asp (20 mM) in a final volume of 150 μL. Then the reaction mixture was incubated at 37 °C for 90 min, and 10 μL of 100% trichloroacetic acid (w/v) was added to stop the reaction. For D-Asp, 1 mM D-Asp was contained in the standard assay mixture. The reaction mixture was incubated for 10 h and then centrifuged. A 75 μL aliquot of the supernatant was then added to the similar solution a final volume of 150 μL, but consisting of 700 nM hDDO. The reaction was stopped after 30 min.

To determine the relative activities of McyF toward L-MetAsp, we also performed assays as previously reported [21]with proper modifications. For L-MetAsp, the standard assay mixture contained McyF (600 nM), sodium pyrophosphate buffer (pH 8.0; 40 mM), and L-MetAsp (50 mM) in a final volume of 150 μL. After centrifugation with 12000 g for 10 min, 90 μL of the supernatant was collected and 10 μL of the ethanol solution containing O-Phthaladehyde and N-acetyl-L-cysteine was added to the supernatant. The mixture was diluted into 10 mL by 0.2 M boric acid buffer (pH 9.8) and vortexed for 5 min, afterwards the samples were flowed through the column of 300SB-C18 (5 μm, 4.6 × 250 mm, Agilent) on HPLC (Agilent Technologies) with the excitation wave length set at 350 nm and quantified by measuring the emission wavelength at 450 nm. And we used the mixture lacking L-MetAsp to be the control. As for the activity towards D-MetAsp, similar procedures were performed, except that 100 mM D-MetAsp was added for each reaction.

## 3. Results

### 3.1. Overall structure of McyF

We determined the crystal structures of seleno-methionine substituted McyF (SeMet-McyF) from *M. aeruginosa* PCC7806 in complex with a citrate at 2.35 Å (Table 1). The full-length McyF was applied for crystallization; however, only the segment of residues Lys4–Lys232 could be traced in the electron density map. The crystal belongs to the space group $P3_221$ and each asymmetric unit of structure contains one molecule (Fig. 1A), although gel-filtration profile indicated that McyF exists as a dimer in solution (data not shown). Indeed, symmetry operation enabled us to define the dimeric structure of McyF in the crystal, with a buried interface area of 1474 $Å^2$, which is sufficient to stabilize a dimer (Fig. 1B). The dimeric interface is mainly stabilized by a cluster of hydrogen

**Table 1**
Crystal parameters, data collection, and structure refinement.

| | SeMet-McyF + Citrate | McyF-C87S/C195S + L-Asp | McyF-C87S/C195S + D-Asp |
|---|---|---|---|
| ***Data collection*** | | | |
| Space group | *$P3_221$* | *P3221* | *P3221* |
| Wavelength (Å) | 0.97930 | 0.97791 | 0.97915 |
| Unit cell parameters | | | |
| *a, b, c* (Å) | 128.75, 128.75, 46.18 | 128.48, 128.48, 45.14 | 129.10, 129.10, 44.64 |
| α, β, γ (°) | 90, 90, 120 | 90, 90, 120 | 90, 90, 120 |
| Resolution range (Å) | 50.0–2.35 (2.39–2.35)[a] | 50.0–2.63 (2.68–2.63) | 50.0–2.80 (2.85–2.80) |
| Unique reflections | 18,567 (913) | 12,847 (630) | 10,736 (521) |
| Completeness (%) | 99.9 (100.0) | 99.7 (99.8) | 99.9 (100.0) |
| $<I/\sigma(I)>$ | 32.4 (6.0) | 21.4 (4.0) | 15.2 (3.4) |
| $R^b_{merge}$ | 0.081 (0.483) | 0.082 (0.493) | 0.086 (0.503) |
| $R_{p.i.m}$ | 0.023 (0.140) | 0.030 (0.176) | 0.044 (0.252) |
| $R_{means}/R_{r.i.m}$ | 0.084 (0.504) | 0.088 (0.526) | 0.097 (0.563) |
| $CC_{1/2}$ | (0.966) | (0.924) | (0.851) |
| Wilson B-factor (Å$^2$) | 46.1 | 47.3 | 58.9 |
| Matthews coefficient (Å$^3$ Da$^{-1}$) | 1.96 | 1.90 | 1.90 |
| Average redundancy | 12.7 (12.6) | 7.8 (7.9) | 4.8 (4.9) |
| ***Phasing statistics*** | | | |
| Anomalous $R_{merge}$ | 0.070 (0.463) | | |
| Anomalous redundancy | 6.6 (6.5) | | |
| Anomalous Completeness (%) | 100 (100) | | |
| Figure of merit | 0.43 | | |
| BAYES-CC | 58.43 | | |
| Model-CC | 0.82 | | |
| ***Structure refinement*** | | | |
| Resolution range (Å) | 50.0–2.35 | 50.0–2.63 | 50.0–2.80 |
| $R^c_{factor}/R^d_{free}$ | 0.187/0.202 | 0.186/0.205 | 0.184/0.203 |
| Number of atoms | | | |
| Protein | 1786 | 1786 | 1786 |
| Water | 79 | 40 | 27 |
| Ligands | 13 | 9 | 9 |
| B factors (Å$^2$) | | | |
| Protein | 49.2 | 49.4 | 61.0 |
| Water | 50.0 | 44.4 | 50.3 |
| Ligands | 50.5 | 47.5 | 73.6 |
| Mean B factors (Å$^2$) | 49.0 | 49.0 | 60.0 |
| RMSD[e] bond lengths (Å) | 0.007 | 0.008 | 0.009 |
| RMSD bond angles (°) | 1.165 | 1.232 | 1.272 |
| ***Validation statistics*** | | | |
| Clash score, all atoms | 1.65 | 0.83 | 1.65 |
| Poor rotamers (%) | 4 | 4 | 7 |
| Ramachandran plot[f] (residues, %) | | | |
| Most favored (%) | 98.22 | 98.22 | 97.33 |
| Additional allowed (%) | 1.78 | 1.78 | 2.67 |
| Outliers (%) | 0 | 0 | 0 |
| **PDB entry** | 5WXX | 5WXY | 5WXZ |

[a]The values in parentheses refer to statistics in the highest bin. [b]$R_{merge} = \sum_{hkl}\sum_i|I_i(hkl) - <I(hkl)>|/\sum_{hkl}\sum_i I_i(hkl)$, where $I_i(hkl)$ is the intensity of an observation and $<I(hkl)>$ is the mean value for its unique reflection; Summations are over all reflections. [c]R-factor $= \sum_h|Fo(h) - Fc(h)|/\sum_h Fo(h)$, where Fo and Fc are the observed and calculated structure-factor amplitudes, respectively. [d]R-free was calculated with 5% of the data excluded from the refinement. [e]Root-mean square-deviation from ideal values. [f]Categories were defined by Molprobity.

bonds between α1, η1, and β2 in subunit A and their counterpart elements in subunit B (Fig. 1B). Noticeably, residue Glu36′ from η1′ of subunit B forms two salt bridges with Arg53 and Lys167 of subunit A, which also contributes to maintaining the dimeric structure (Fig. 1B).

### 3.2. The catalytic pocket of McyF

McyF shares an overall structure similar to other aspartate racemases, such as *Ph*AspR from *Pyrococcus horikoshii* OT3 [6,22] and *Pto*AspR from *Picrophilus torridus* [23], with a root-mean-square deviation (RMSD) of approximately 2.2–2.3 Å. In the SeMet-McyF structure, a citrate molecule occupies the catalytic pocket, which is located at the cleft between two domains (Fig. 1A). The active-site pocket is composed of α2 (Asp52, Arg53, Thr54), η2 (Cys87, Cys88, Thr89), α7 (Ile162, Tyr163), and the connection loops of β1-α1 (Met14), β4-α5 (Ser128), α7-η5 (Lys167), and β6-α9 (Cys195, Thr196, Glu197) (Fig. 2A). Notably, Cys87 and Cys195 are catalytic residues responsible for the interconversion of L-Asp and D-Asp, as deduced from previous reports [24]. The side-chains of residues Arg53, Thr54, Thr89, Ser128, Tyr163, Lys167, Cys195, Thr196, and Glu197 form 19 hydrogen bonds with the citrate molecule. Structure-based multiple-sequence alignment showed that these residues are highly conserved in McyF and homologs from a variety of species (Fig. 1C).

To elucidate the structural basis of catalytic mechanism and substrate specificity of McyF, we solved the structures of McyF-C87S/C195S in complex with the substrates L-Asp and D-Asp (Table 1), respectively. Eight residues participate in the interaction with substrate L-Asp or D-Asp. Apart from two catalytic cysteines Cys87 and Cys195, residues Met14, Arg53, Cys88, Thr89, Lys167, Thr196, and Glu197 are responsible for stabilizing the substrate via hydrogen bonds or hydrophobic interactions (Fig. 2B and C). In addition, multiple-sequence alignment revealed all substrate-binding residues are highly conserved (Fig. 1C). Notably, residues Arg53 and Lys167 of subunit A form two hydrogen bonds with the

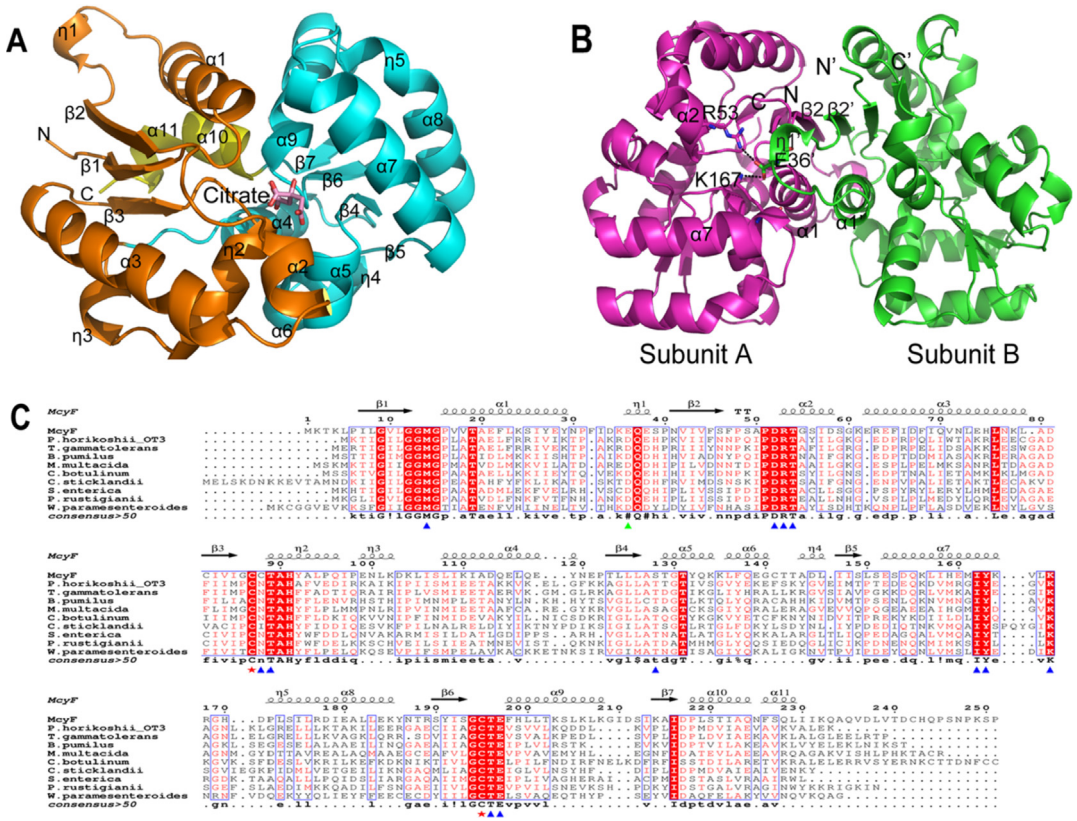


**Fig. 1.** The overall structure of McyF. (**A**) Ribbon diagrams of the monomer structure of McyF. (**B**) Ribbon diagrams of the dimer structure of McyF. (**C**) Structure-based multiple-sequence alignment of McyF and homologs from diverse species. Catalytic residues Cys87 and Cys195 are indicated with red stars. Residues interact with citrate are shown with blue triangle. Residue E36 shown in green triangle is involved in the stabilization of active-site pocket. All sequences were downloaded from the NCBI database.

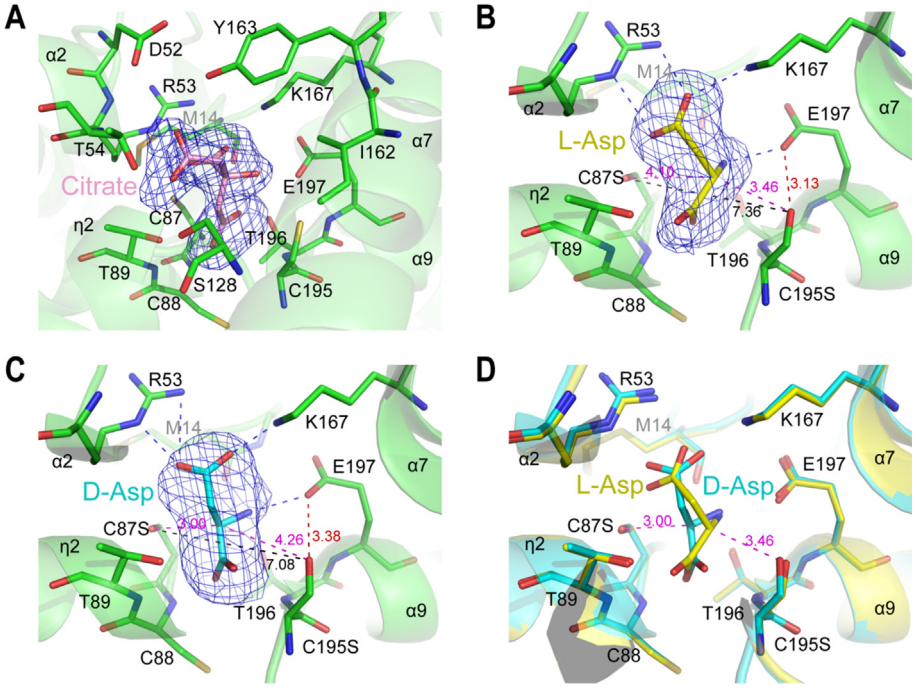


**Fig. 2.** The active-site pocket of McyF. The active-site pocket of McyF in complex with citrate (**A**), L-Asp (**B**) and D-Asp (**C**). The involved residues are shown in green sticks, and the ligands are shown as sticks in different colors. The polar interactions are indicated by blue dashed lines. The simulated annealing $|Fo|-|Fc|$ difference electron density maps of ligands contoured at 3.0 $\sigma$ are shown as blue mesh. (**D**) Structural superposition of McyF-C87S/C195S-L-Asp against McyF-C87S/C195S-D-Asp. McyF-C87S/C195S-L-Asp and McyF-C87S/C195S-D-Asp are shown in yellow and cyan, respectively.

residue Glu36′ from η1′ of subunit B, also contributing to the formation of catalytic pocket (Fig. 1B).

The simulated annealing |*Fo*|−|*Fc*| difference electron density maps contoured at 3.0 σ clearly showed the density of citrate, L-Asp and D-Asp (Fig. 2A–2C). In the crystal structure of McyF-C87S/C195S-L-Asp, the hydrogen atom linked to the Cα of L-Asp is proposed to orient towards the hydroxyl group of mutated Ser195. A distance of 3.46 Å between the Cα atom of L-Asp and the oxygen atom in the hydroxyl group of Ser195 is reasonable to launch the nucleophilic attack for deprotonation (Fig. 2B). In contrast, the hydrogen atom in Cα atom of D-Asp orients towards the hydroxyl group of Ser87 in structure of mutant McyF-C87S/C195S-D-Asp, with a distance of 3.00 Å between the Cα and oxygen atoms (Fig. 2C). Structural superposition of McyF-C87S/C195S-L-Asp against McyF-C87S/C195S-D-Asp clearly showed the interconversion of L-Asp and D-Asp (Fig. 2D). The structures of McyF-C87S/C195S in complex with the substrate L-Asp or D-Asp enabled us to assign Cys87 and Cys195 as the proposed "two bases" to perform the deprotonation of D-Asp and L-Asp, respectively [6,25].

### 3.3. Glu197 plays a crucial role in catalysis

To investigate the catalytic mechanism of McyF, we performed the site-directed mutagenesis combined with *in vitro* aspartate racemization activity assays. Only the racemization activities of wild-type McyF and C195S mutant towards L-Asp were detectable when we measured the kinetic parameters of McyF and its mutants (Table 2). Except for wild-type McyF and C195S mutant, only mutant E197Q showed little racemization activity towards either L-Asp or D-Asp even though the reactions were performed overnight. As predicted, McyF is capable of catalyzing the interconversion of L-Asp and D-Asp (Fig. 3A and B). The mutant McyF-C87S completely lost the racemization activity towards either L-Asp or D-Asp, whereas the mutant McyF-C195S remained about 10–20% residual racemization activity compared to the wild-type (Fig. 3A and B). The activity loss of McyF-C87S suggested that the hydroxyl group of serine was much less reactive compared to the thiol group of cysteine. The difference between Cys87 and Cys195 prompted us to comprehensively compare their surrounding residues, and we found that Cys195 is further stabilized by an acid residue Glu197 (Fig. 2B and C). Subsequent single mutation of E197Q or double mutations of C195S/E197Q led to a sharp decrease or complete loss of the racemization activity (Fig. 3A and B), suggesting the collaboration of Cys195 and Glu197 during the interconversion reaction of L-Asp and D-Asp.

### 3.4. McyF is capable to catalyze the racemization of MeAsp

McyF is encoded by *mcyF* gene which belongs to the *mcy* gene cluster that consists of ten genes involved in the biosynthesis of microcystins in *M. aeruginosa* PCC7806 [9]. Two isoforms of microcystin have been reported in *M. aeruginosa* PCC7806, which employ either D-Asp or D-MeAsp as the precursor [12]. As we know, D-Asp is generated from L-Asp by the aspartate racemase McyF [9,10]; however, the biosynthesis of D-MeAsp has never been elucidated. The intracellular L-MeAsp is a key component in the biosynthesis pathway of C5-branched dibasic acid metabolism & glyoxylate and dicarboxylate metabolism (KEGG: http://www.genome.jp/kegg/). It is known that the reversible isomerization of L-MeAsp and L-glutamate is catalyzed by the glutamate mutase (*EC 5.4.99.1*) [26], whereas the reversible addition of ammonia to mesaconate to yield L-MeAsp is catalyzed by the methyl-aspartate ammonia-lyase (*EC 4.3.1.2*) [27]. The enrichment of L-MeAsp implies that it probably serves as the precursor of D-MeAsp catalyzed by a racemase. In addition, McyF is the only aspartate racemase encoded by *M. aeruginosa* PCC 7806 genome, strongly suggesting McyF could also catalyze the conversion of L-MeAsp to D-MeAsp. To prove this assumption, we chemically synthesized L-MeAsp and D-MeAsp and performed the activity assays, respectively. The activity towards MeAsp is relatively low but detectable. For the racemic reaction on L-MeAsp, the production of D-MeAsp can be detected after 3 h incubated at 37 °C compared to the control group (Fig. 4A). Apparent increasing production of D-MeAsp can be detected after the reaction was prolonged to 10 h. On the contrary, reactions towards D-MeAsp was rather weak. Slight production of L-MeAsp could be detected after a reaction for 10 h (Fig. 4B). However, for the first time, our essays proved that McyF could also catalyze the interconversion of L-MeAsp and D-MeAsp, the precursor of another microcystin isoform.

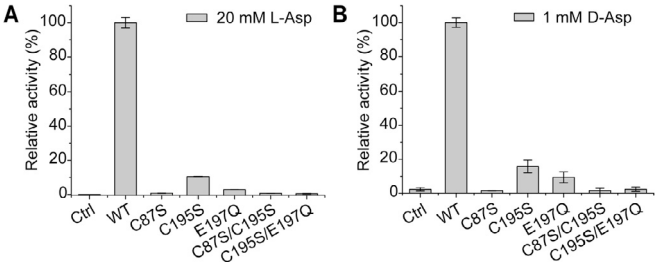


**Fig. 3.** The relative activities of McyF towards aspartate and mutants and sequence alignment of McyF and homologs. The relative activities of McyF and mutants toward 20 mM L-Asp (**A**) and 1 mM D-Asp (**B**). All experiments were performed in triplicate.

**Table 2**
The kinetic parameters of McyF and its mutants towards L-Asp.

| Enzyme | $K_m$ (mM) | $k_{cat}$ ($s^{-1}$) | $k_{cat}/K_m$ ($s^{-1}$ $mM^{-1}$) |
|---|---|---|---|
| Wild type | 22.9 ± 2.1 | 42.5 ± 1.3 | 1.86 |
| C87S | ND[a] | ND | ND |
| C195S | 61.5 ± 7.4 | 1.64 ± 0.09 | 2.67e-2 |
| C87S/C195S | ND | ND | ND |
| E197Q | ND | ND | ND |
| C195S/E197Q | ND | ND | ND |

[a] The activity cannot be detected.

## 4. Discussion

We solved three crystal structures of McyF in complex with the substrates or analogues. Structural analyses combined with activity assays enabled us to clearly assign the substrate-binding and catalytic residues. The racemization activity assays combined with structural analyses illustrated the substrate specificity of McyF and provide insight into the catalytic mechanism of the aspartate racemase. The biochemical assays proved that McyF is capable of catalyzing the interconversion of L-MeAsp and D-MeAsp, thus also participate in the biosynthesis of another microcystin isoform. However, further structural information and biochemical characterization are needed to comprehensively elucidate the biosynthesis pathway of cyanobacterial microcystin.

## Statement of conflict of interest

The authors declare no conflict of interest.

## Author contributions

D.D.C., C.P.Z, Y.C., and C.Z.Z. designed the study; D.D.C. and C.P.Z performed experiments; D.D.C., K.Z., Y.L.J., X.F.T., J.X., Y.C., C.Z.Z. and

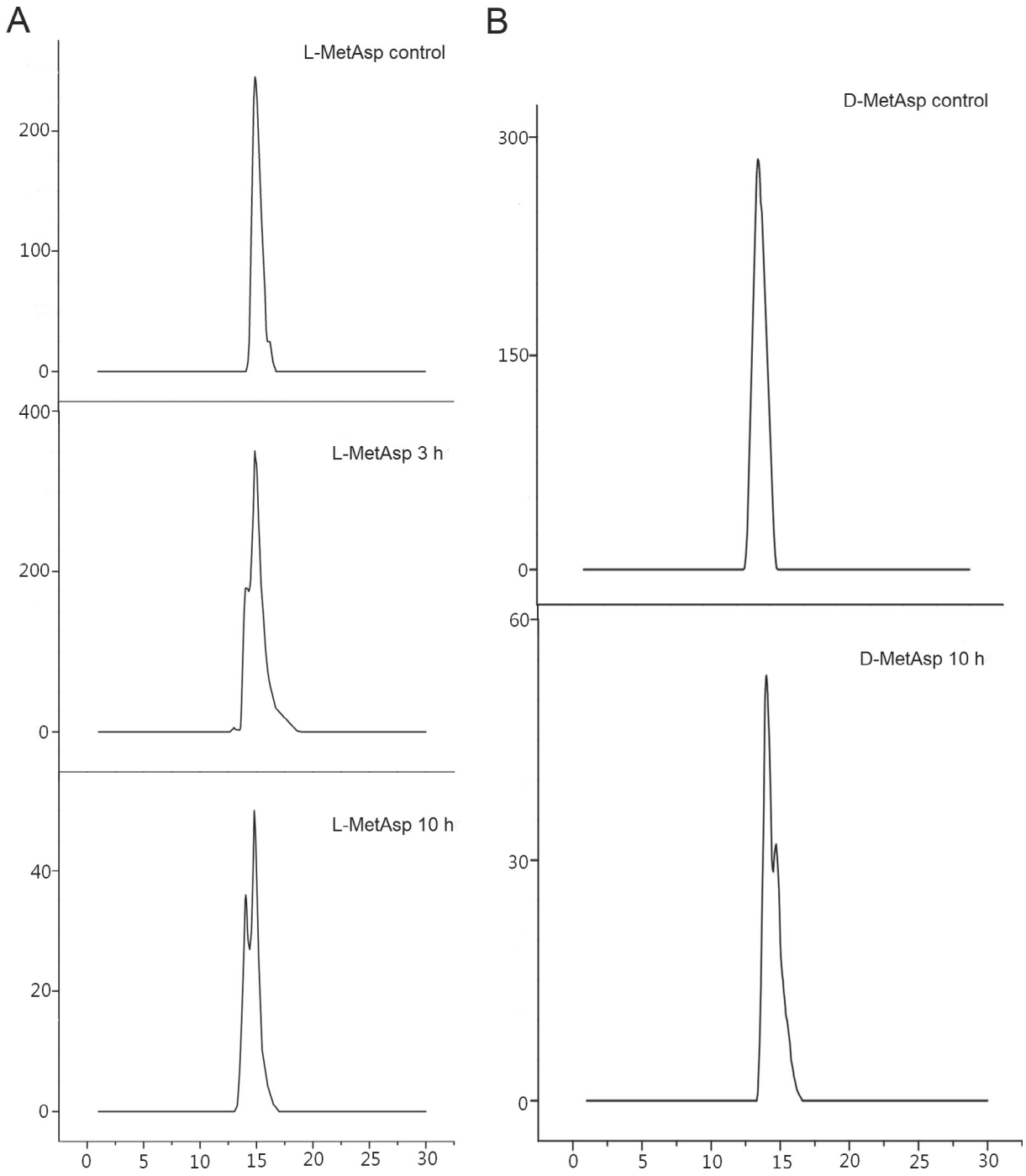


**Fig. 4.** Biochemical assays for the activities of MycF towards D-MeAsp and L-MeAsp using HPLC (**A**) The relative activities of MycF towards L-MetAsp (**B**) The activity of McyF towards D-MetAsp.

W.T.H analyzed the data; Y.M.R. provided reagents; D.D.C., Y.C., C.Z.Z. and W.T.H wrote the manuscript.

## Acknowledgments

We thank Rui-Han Dai from School of Chemistry and Materials Science, University of Science and Technology of China for the synthesis of L-/D-MetAsp. This work was supported by National Natural Science Foundation of China (Grants No. 31630001, 31370757, and 31500602), and Ministry of Education of the People's Republic of China (Grant No. 20133402110023). We appreciate the assistance of the staff at the Shanghai Synchrotron Radiation Facility (SSRF) and the Core Facility Center for Life Sciences in University of Science and Technology of China. We are grateful to all of the developers of the CCP4 Suite, PyMOL, PHENIX, and ESPript.

## References

[1] J. van Heijenoort, Formation of the glycan chains in the synthesis of bacterial peptidoglycan, Glycobiology 11 (2001) 25r–36r.
[2] J. van Heijenoort, Recent advances in the formation of the bacterial peptidoglycan monomer unit, Nat. Prod. Rep. 18 (2001) 503–519.
[3] M. Katane, H. Homma, D.- Aspartate Oxidase, The sole catabolic enzyme acting

on free D-aspartate in mammals, Chem. Biodivers. 7 (2010) 1435–1449.
[4] H. Wolosker, E. Dumin, L. Balan, V.N. Foltyn, D-amino acids in the brain: D-serine in neurotransmission and neurodegeneration, FEBS J. 275 (2008) 3514–3526.
[5] A. Buschiazzo, M. Goytia, F. Schaeffer, W. Degrave, W. Shepard, C. Gregoire, N. Chamond, A. Cosson, A. Berneman, N. Coatnoan, P.M. Alzari, P. Minoprio, Crystal structure, catalytic mechanism, and mitogenic properties of Trypanosoma cruzi proline racemase, Proc. Natl. Acad. Sci. U.S.A. 103 (2006) 1705–1710.
[6] A. Ohtaki, Y. Nakano, R. Iizuka, T. Arakawa, K. Yamada, M. Odaka, M. Yohda, Structure of aspartate racemase complexed with a dual substrate analogue, citric acid, and implications for the reaction mechanism, Proteins 70 (2008) 1167–1174.
[7] J.W. Ahn, J.H. Chang, K.J. Kim, Structural basis for an atypical active site of an L-aspartate/glutamate-specific racemase from Escherichia coli, FEBS Lett. 589 (2015) 3842–3847.
[8] X. Liu, F. Gao, Y. Ma, S. Liu, Y. Cui, Z. Yuan, X. Kang, Crystal structure and molecular mechanism of an aspartate/glutamate racemase from Escherichia coli O157, FEBS Lett. 590 (2016) 1262–1269.
[9] D. Tillett, E. Dittmann, M. Erhard, H. von Dohren, T. Borner, B.A. Neilan, Structural organization of microcystin biosynthesis in Microcystis aeruginosa PCC7806: an integrated peptide-polyketide synthetase system, Chem. Biol. 7 (2000) 753–764.
[10] X.F. Tan, Y.N. Dai, K. Zhou, Y.L. Jiang, Y.M. Ren, Y. Chen, C.Z. Zhou, Structure of the adenylation-peptidyl carrier protein didomain of the Microcystis aeruginosa microcystin synthetase McyG, Acta crystallographica. Section D, Biological crystallography 71 (2015) 873–881.
[11] H. Sielaff, E. Dittmann, N. Tandeau De Marsac, C. Bouchier, H. Von Dohren, T. Borner, T. Schwecke, The mcyF gene of the microcystin biosynthetic gene cluster from Microcystis aeruginosa encodes an aspartate racemase, Biochem. J. 373 (2003) 909–916.
[12] R. Dierstein, I. Kaiser, J. Weckesser, U. Matern, W.A. König, R. Krebber, Two closely related peptide toxins in axenically grown *Microcystis aeruginosa* PCC-7806, Syst. Appl, An. Microbiol. 13 (1990) 86–91.
[13] H. Walden, Selenium incorporation using recombinant techniques, Acta Crystallogr. D 66 (2010) 352–357.
[14] Z. Otwinowski, W. Minor, Processing of X-ray diffraction data collected in oscillation mode, Methods Enzymol. 276 (1997) 307–326.
[15] P.D. Adams, P.V. Afonine, G. Bunkoczi, V.B. Chen, I.W. Davis, N. Echols, J.J. Headd, L.W. Hung, G.J. Kapral, R.W. Grosse-Kunstleve, A.J. McCoy, N.W. Moriarty, R. Oeffner, R.J. Read, D.C. Richardson, J.S. Richardson, T.C. Terwilliger, P.H. Zwart, PHENIX: a comprehensive Python-based system for macromolecular structure solution, Acta Crystallogr. D 66 (2010) 213–221.
[16] M.D. Winn, C.C. Ballard, K.D. Cowtan, E.J. Dodson, P. Emsley, P.R. Evans, R.M. Keegan, E.B. Krissinel, A.G.W. Leslie, A. McCoy, S.J. McNicholas, G.N. Murshudov, N.S. Pannu, E.A. Potterton, H.R. Powell, R.J. Read, A. Vagin, K.S. Wilson, Overview of the CCP4 suite and current developments, Acta Crystallogr. D 67 (2011) 235–242.
[17] P. Emsley, B. Lohkamp, W.G. Scott, K. Cowtan, Features and development of coot, Acta Crystallogr. D 66 (2010) 486–501.
[18] V.B. Chen, W.B. Arendall, J.J. Headd, D.A. Keedy, R.M. Immormino, G.J. Kapral, L.W. Murray, J.S. Richardson, D.C. Richardson, MolProbity: all-atom structure validation for macromolecular crystallography, Acta Crystallogr. D 66 (2010) 12–21.
[19] R.A. Laskowski, M.W. Macarthur, D.S. Moss, J.M. Thornton, Procheck - a program to check the stereochemical quality of protein structures, J. Appl. Crystallogr. 26 (1993) 283–291.
[20] M. Katane, K. Nakayama, T. Kawata, Y. Yokoyama, Y. Matsui, Y. Kaneko, S. Matsuda, Y. Saitoh, T. Miyamoto, M. Sekine, H. Homma, A sensitive assay for measuring aspartate-specific amino acid racemase activity, J. Pharm. Biomed. Anal. 116 (2015) 109–115.
[21] S. Einarsson, B. Josefsson, P. Moller, D. Sanchez, Separation of amino-acid enantiomers and chiral amines using precolumn derivatization with (+)-1-(9-Fluorenyl)Ethyl chloroformate and reversed-phase liquid-chromatography, Anal. Chem. 59 (1987) 1191–1195.
[22] L. Liu, K. Iwata, A. Kita, Y. Kawarabayasi, M. Yohda, K. Miki, Crystal structure of aspartate racemase from Pyrococcus horikoshii OT3 and its implications for molecular mechanism of PLP-independent racemization, J. Mol. Biol. 319 (2002) 479–489.
[23] T. Aihara, T. Ito, Y. Yamanaka, K. Noguchi, M. Odaka, M. Sekine, H. Homma, M. Yohda, Structural and functional characterization of aspartate racemase from the acidothermophilic archaeon Picrophilus torridus, Extremophiles : Life Under Extreme Conditions 20 (2016) 385–393.
[24] T. Yoshida, T. Seko, O. Okada, K. Iwata, L.J. Liu, K. Miki, M. Yohda, Roles of conserved basic amino acid residues and activation mechanism of the hyperthermophilic aspartate racemase at high temperature, Proteins-Structure Function and Bioinformatics 64 (2006) 502–512.
[25] S. Glavas, M.E. Tanner, Catalytic acid/base residues of glutamate racemase, Biochemistry-Us 38 (1999) 4106–4113.
[26] E.N. Marsh, Review article coenzyme-B(12)-dependent glutamate mutase, Bioorg. Chem. 28 (2000) 176–189.
[27] S.K. Goda, N.P. Minton, N.P. Botting, D. Gani, Cloning, sequencing, and expression in Escherichia coli of the Clostridium tetanomorphum gene encoding beta-methylaspartase and characterization of the recombinant protein, Biochemistry-Us 31 (1992) 10747–10756.